Mgr2 regulates mitochondrial preprotein import by associating with channel-forming Tim23 subunit

Srujan Kumar Matta, Abhishek Kumar, and Patrick D'Silva*
Department of Biochemistry, New Biological Sciences Building, Indian Institute of Science, Bangalore-560012, India

ABSTRACT **Mgr2, a newly identified subunit of the TIM23 complex, functions as a gatekeeper of presequence translocase and thereby maintains quality control of inner membrane preproteins sorting. However, precise recruitment of the Mgr2 subunit to the core channel and how it influences the assembly of the TIM23 complex during lateral sorting of preproteins are poorly understood. Present findings provide insights into a direct association of Mgr2 with the channel-forming Tim23 subunit. Furthermore, the mutational analysis uncovers the TM1 region of Mgr2 critically required for association with Tim23 and Tim21. On the other hand, the TM2 region of Mgr2 is involved in bridging respiratory complexes to the TIM23 complex via Tim21. Importantly, both TM regions of Mgr2 are essential for lateral sorting of preprotein into the inner membrane, as well as maintaining mitochondrial morphology. Together, our findings provide mechanistic insights into the role of Mgr2 in regulating the dynamicity of the TIM23 complex assembly required for preprotein import and coupling of respiratory pathways.**

Monitoring Editor
Thomas Fox
Cornell University

Received: Dec 5, 2019
Revised: Feb 27, 2020
Accepted: Mar 13, 2020

INTRODUCTION

The majority of the mitochondrial proteome is nuclear encoded and synthesized on cytosolic ribosomes as preproteins. The TOM complex (translocase of the outer membrane) acts as a general entry gate for all the incoming preproteins (Truscott *et al.*, 2003; Baker *et al.*, 2007; Chacinska *et al.*, 2009; Schmidt *et al.*, 2010; van der Laan *et al.*, 2010; Schulz *et al.*, 2015; Wiedemann and Pfanner, 2017; Kang *et al.*, 2018; Araiso *et al.*, 2019; Pfanner *et al.*, 2019). Once emerged from the TOM complex, precursor proteins with N-terminal presequence are imported by the TIM23 complex (translocase of the inner membrane) attributing to ~70% of the mitochondrial proteome (Baker *et al.*, 2007; Neupert and Herrmann, 2007; Chacinska *et al.*, 2009; van der Laan *et al.*, 2010; Wiedemann and Pfanner, 2017; Kang *et al.*, 2018; Pfanner *et al.*, 2019). To perform such a discrete task, the TIM23 complex undergoes dynamic switching between MOTOR and SORT states of the complex during preprotein translocation. The $TIM23^{MOTOR}$ complex is involved in the import of matrix resident proteins. On the other hand, the $TIM23^{SORT}$ complex facilitates the lateral sorting of preproteins into the inner membrane of mitochondria (Chacinska *et al.*, 2005; Neupert and Herrmann, 2007; Schulz *et al.*, 2015; Schendzielorz *et al.*, 2018; Araiso *et al.*, 2019; Pfanner *et al.*, 2019). The core of the TIM23 complex consists of three essential proteins: Tim23, Tim17, and Tim50 (Dekker *et al.*, 1993; Emtage and Jensen, 1993; Maarse *et al.*, 1994; Ryan *et al.*, 1994; Bauer *et al.*, 1996; Yamamoto *et al.*, 2002; Mokranjac *et al.*, 2003; Wiedemann and Pfanner, 2017). Tim23 is a multi-spanning integral membrane protein that forms the core of the voltage-gated channel (Dekker *et al.*, 1993; Kubrich *et al.*, 1994; Bauer *et al.*, 1996; Alder *et al.*, 2008; de la Cruz *et al.*, 2010; Pareek *et al.*, 2013). On the other hand, Tim17 is required for the regulation of the gating and architecture of the core channel (Maarse *et al.*, 1994; Meier *et al.*, 2005; Martinez-Caballero *et al.*, 2007; Ramesh *et al.*, 2016; Demishtein-Zohary *et al.*, 2017; Matta *et al.*, 2017). Tim50 assists in the initial recognition of the preproteins emerging from the TOM complex

This article was published online ahead of print in MBoC in Press (http://www.molbiolcell.org/cgi/doi/10.1091/mbc.E19-12-0677) on March 18, 2020.

The authors declare that they have no conflict of interest.

Author contributions: S.K.M., A.K., and P.D. designed experiments and analyzed the data; S.K.M. performed experiments; S.K.M., A.K., and P.D. wrote the manuscript.

*Address correspondence to: Patrick D'Silva (patrick@iisc.ac.in).

Abbreviations used: BSA, bovine serum albumin; DHFR, dihydrofolate reductase; Co-IP, coimmunoprecipitation; IPTG, isopropyl 1-thio-β-D-galactopyranoside; PK, proteinase K; PMSF, phenylmethylsulfonyl fluoride; ROMO, reactive oxygen species modulator; TIM, translocase of the inner membrane; TM, transmembrane; TOM, translocase of the outer membrane.

(Geissler *et al.*, 2002; Tamura *et al.*, 2009; Marom *et al.*, 2011; Bajaj *et al.*, 2014; Li and Sha, 2015; Dayan *et al.*, 2019). The initial import is driven by a membrane potential (ψ) difference across the inner membrane; however, the complete translocation into the matrix requires $TIM23^{MOTOR}$ complex (Martin *et al.*, 1991; Bauer *et al.*, 1996; Truscott *et al.*, 2001; Alder *et al.*, 2008; van der Laan *et al.*, 2010; Denkert *et al.*, 2017; Schendzielorz *et al.*, 2017). The mtHsp70 is the central component of $TIM23^{MOTOR}$ complex and functions in the vectorial import of preproteins in an ATP hydrolysis-dependent manner (Berthold *et al.*, 1995; Geissler *et al.*, 2001; Liu *et al.*, 2003; D'Silva *et al.*, 2004; De Los Rios *et al.*, 2006; Baker *et al.*, 2007). Pam18 and Pam16 belong to the J-/J-like class of cochaperones that aid in regulating the ATPase activity of mtHsp70 (D'Silva *et al.*, 2003, 2005, 2008; Frazier *et al.*, 2004; Kozany *et al.*, 2004). Tim44 acts as a scaffold for import motor tethering onto the $TIM23^{CORE}$ complex (D'Silva *et al.*, 2004, 2008; Baker *et al.*, 2007; Schiller, 2009; Banerjee *et al.*, 2015; Ting *et al.*, 2017).

$TIM23^{SORT}$ complex consists of two additional proteins, Mgr2 and Tim21 (Chacinska *et al.*, 2005; Gebert *et al.*, 2012; Pfanner *et al.*, 2019). Tim21 operates at the TOM-TIM transit site during preprotein import. Furthermore, Tim21 mediates the coupling of the TIM23 complex with respiratory complexes by transiently associating with complex III and IV (Chacinska *et al.*, 2005; Mokranjac *et al.*, 2005; Albrecht *et al.*, 2006; van der Laan *et al.*, 2006; Wiedemann *et al.*, 2007; Gebert *et al.*, 2012). Mgr2 is a recently identified subunit of the TIM23 complex consisting of two predicted transmembrane (TM) regions (Gebert *et al.*, 2012). Mgr2 functions as a gatekeeper for maintaining the quality control of laterally sorted preproteins by delaying their release into the inner membrane (Ieva *et al.*, 2014). Additionally, Mgr2 aids in the recruitment of Tim21 to the TIM23 complex and thereby aids in bridging respiratory complexes with translocase (Gebert *et al.*, 2012). Moreover, Mgr2 regulates the structural dynamics of mitochondria through proper biogenesis of fusion protein Mgm1 (Ieva *et al.*, 2014). ROMO1 (reactive oxygen species modulator), the human orthologue of Mgr2, was shown to be a part of the mammalian TIM23 complex and required for OXPHOS assembly via Tim21 (Richter *et al.*, 2019). Surprisingly, ROMO1−/− cells displayed severely reduced import of i-AAA protease YME1L, thereby influencing the mitochondrial structures through defective processing of OPA1 (Mgm1 orthologue) (Richter *et al.*, 2019). Furthermore, ROMO1 is implicated in several cancers due to its regulatory role in reactive oxygen species production and apoptosis (Chung *et al.*, 2006, 2008, 2012; Na *et al.*, 2008; Shin *et al.*, 2013; Kim *et al.*, 2014, 2017; Norton *et al.*, 2014; Swarnabala *et al.*, 2014; Lee *et al.*, 2015). Interestingly, recent findings using patch-clamp electrophysiology suggested that the deletion of Mgr2 affects the gating behavior of the TIM23 complex; thus, it is conceivable that Mgr2/ROMO1 could form the part of the active protein-conducting channel (Mirzalieva *et al.*, 2019). However, the precise recruitment of Mgr2 at the TIM23 core channel, together as a subcomplex with Tim21 and how it regulates preprotein import, channel gating, and mitochondrial dynamics, is still an open question. By utilizing several biochemical and genetic approaches, the current study highlights the role of different regions of Mgr2 required for the dynamicity of presequence translocase assembly and in coupling the protein import machinery to the respiratory pathways.

RESULTS AND DISCUSSION

Mgr2 directly associates with the channel-forming Tim23 subunit

The interaction of Mgr2 with the transiting preprotein at the import channel is considered a rate-limiting step during the lateral sorting of preproteins (Gebert *et al.*, 2012; Ieva *et al.*, 2014; Mirzalieva *et al.*, 2019). However, the precise recruitment of Mgr2 to the TIM23 channel is still enigmatic. Recent findings using patch clamping studies indicated that the deletion of Mgr2 affects the TIM23 channel gating (Mirzalieva *et al.*, 2019), thereby raising the possibility of Mgr2 being directly recruited by Tim23 to the import channel. To test this hypothesis, we purified full-length $Tim23_{HIS}$ and GST-Mgr2 proteins, confirmed their purity by SDS–PAGE, followed by immunoblotting (Figure 1A and Supplemental Figure S1A). To test the direct interaction, in vitro GST–pull-down assay was performed. Remarkably, $Tim23_{HIS}$ exhibited a significant interaction with GST-Mgr2 in a concentration-dependent manner (Figure 1B). GST alone incubated with $Tim23_{HIS}$ served as a negative control to rule out nonspecific binding (Figure 1B). To further support in vitro findings, mitochondria lysed with Triton X-100 (for complete dissociation of the TIM23 complex) was incubated with purified GST-Mgr2 protein followed by pull-down analysis to examine the binding of individual components of the TIM23 complex. In accordance with our in vitro observations, Tim23 efficiently copurified with GST-Mgr2 (Figure 1C). Additionally, we observed specific binding of GST-Mgr2 with Tim21, further ascertaining the role of Mgr2 in coupling Tim21 to the TIM23 complex (Figure 1C). Moreover, GST-Mgr2 failed to interact with other subunits of the TIM23 complex including Tim17, Tim50, Tim44, Pam18, Pam16, and the TOM complex subunit Tom70, thus confirming the specificity of binding of Mgr2 with Tim23 and Tim21 (Figure 1C). To further validate the above observations, we performed a pull down with $Tim21_{HA}$. Interestingly, GST-Mgr2 and Tim23 efficiently copurified with $Tim21_{HA}$, but not other components of the TIM23 complex, thus validating the dual interaction of Mgr2 with Tim23 and Tim21 (Figure 1D). Since Mgr2 recruits Tim21 to the TIM23 complex, we tested whether they exist as a stable subcomplex in vivo. The pull-down analysis with $Tim21_{HA}$ in Triton X-100-lysed mitochondrial extracts revealed that Mgr2 and Tim21 do not exist as a stable subcomplex in vivo; however, Mgr2 might be having differential interactions with Tim23 and Tim21 (Supplemental Figure S1B). In summary, these findings provide direct evidence for the association of Mgr2 with Tim23 subunit.

Mutation in the Tim23 TM2 region (G145L) caused the displacement of Mgr2 from the TIM23 complex, leading to defective channel gating (Mirzalieva *et al.*, 2019). Therefore, to determine the direct link between Mgr2 and TM2 region of Tim23, we tested for a synthetic growth phenotype in the presence of a $tim23_{G149E}$ mutant (mutation resides within the TM2 region of Tim23). Surprisingly, the deletion of *mgr2* in the $tim23_{G149E}$ mutant alleviated the growth sensitivity of the cells compared with the mutant alone (Supplemental Figure S2A). On the contrary, overexpression of Mgr2 was able to partially suppress the growth sensitivity of the $tim23_{G149E}$mutant (Supplemental Figure S2B). To gain further insights, we performed coimmunoprecipitation (Co-IP) in mitochondrial lysates from wild-type, *mgr2*Δ, and $tim23_{G149E}$ yeast strains using anti-Tim23 antibodies. Strikingly, the $tim23_{G149E}$ mutant exhibited impairment in the interaction with Mgr2. This further abrogated the recruitment of Tim21 to TIM23 complex (Figure 1E). As anticipated, the deletion of *mgr2* caused the displacement of Tim21 from the TIM23 complex, but the association of Tim50 with Tim23 remained unaltered in all mutants (Figure 1E). At the same time, the $tim23_{G149E}$ mutant showed impaired recruitment of Tim17 in agreement with previous findings (Figure 1E) (Pareek *et al.*, 2013). To establish a direct role of the Tim23 TM2 region in mediating Mgr2 interaction, we analyzed the binding of purified GST-Mgr2 with mutant $Tim23_{HIS}$-G149E by in vitro GST–pull-down analysis. Interestingly, the mutant $Tim23_{HIS}$-G149E showed a significant impairment in the interaction with

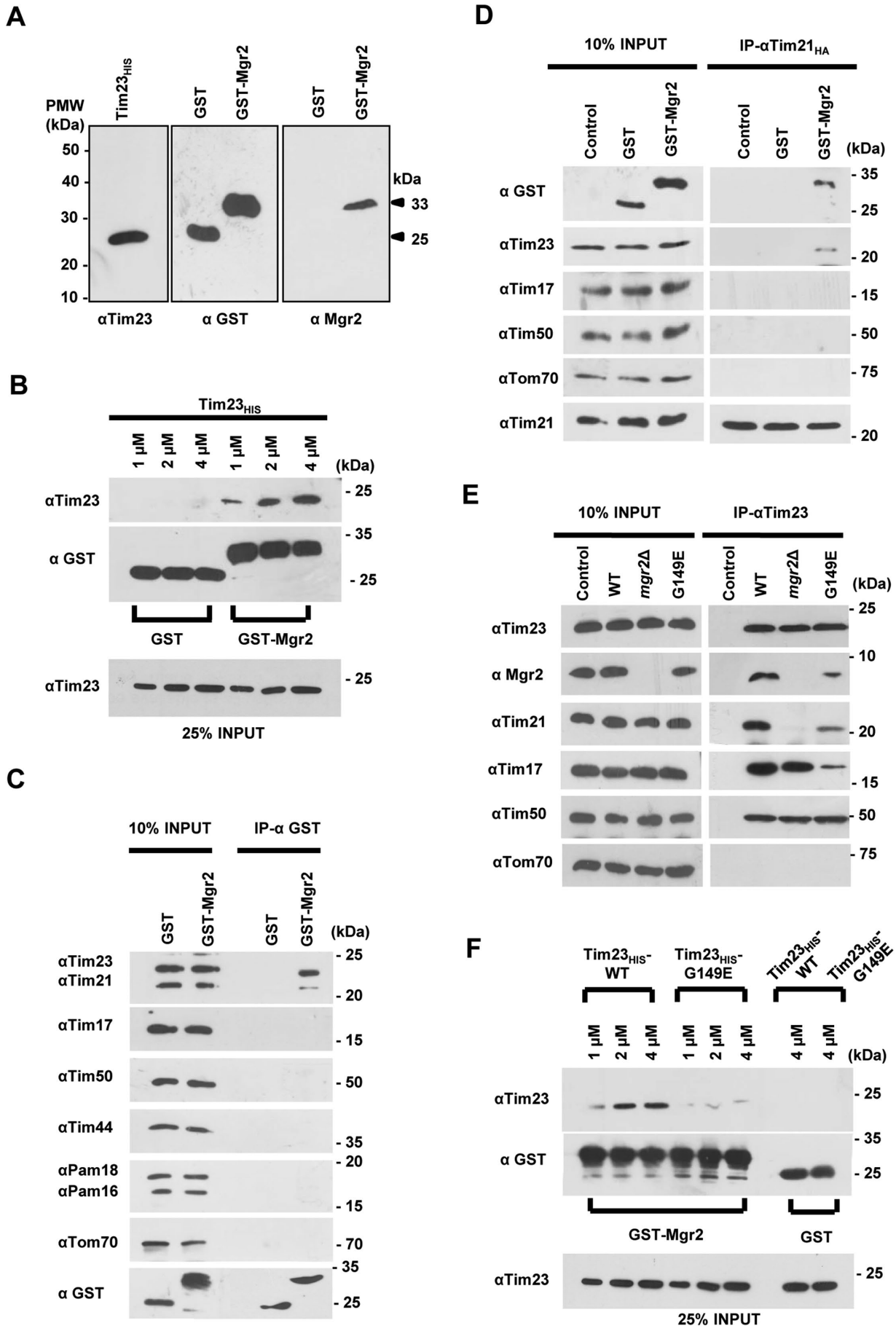
A
PMW (kDa)
Tim23HIS
GST
GST-Mgr2
GST
GST-Mgr2
50
40
30
20
10
kDa
33
25
αTim23
α GST
α Mgr2
B
Tim23HIS
1 μM
2 μM
4 μM
1 μM
2 μM
4 μM
(kDa)
αTim23
- 25
α GST
- 35
- 25
GST
GST-Mgr2
αTim23
- 25
25% INPUT
C
10% INPUT
IP-α GST
GST
GST-Mgr2
GST
GST-Mgr2
(kDa)
αTim23
αTim21
- 25
- 20
αTim17
- 15
αTim50
- 50
αTim44
- 35
αPam18
αPam16
- 20
- 15
αTom70
- 70
α GST
- 35
- 25
D
10% INPUT
IP-αTim21HA
Control
GST
GST-Mgr2
Control
GST
GST-Mgr2
(kDa)
α GST
- 35
- 25
αTim23
- 20
αTim17
- 15
αTim50
- 50
αTom70
- 75
αTim21
- 20
E
10% INPUT
IP-αTim23
Control
WT
mgr2Δ
G149E
Control
WT
mgr2Δ
G149E
(kDa)
αTim23
- 25
α Mgr2
- 10
αTim21
- 20
αTim17
- 15
αTim50
- 50
αTom70
- 75
F
Tim23HIS-WT
Tim23HIS-G149E
Tim23HIS-WT
Tim23HIS-G149E
1 μM
2 μM
4 μM
1 μM
2 μM
4 μM
4 μM
4 μM
(kDa)
αTim23
- 25
α GST
- 35
- 25
GST-Mgr2
GST
αTim23
- 25
25% INPUT

GST-Mgr2 as compared with wild type, thus highlighting the role of TM2 region of Tim23 in the recruitment of Mgr2 to the import channel (Figure 1F). In conclusion, it is reasonable to believe that the binding of Mgr2 to the TM2 region of Tim23 may induce structural changes to the TIM23 core channel, since this segment is shown to undergo voltage-coupled conformational changes (Alder *et al.*, 2008), thus playing a critical role in channel gating during the preprotein import.

Conserved motifs in the TM regions of Mgr2 play a critical role in cellular viability

Mgr2 belongs to the same family of Tim23/Tim17 protein transporters and thus shares a significant similarity in the organization of TM domains (Zarsky and Dolezal, 2016). These classes of proteins possess characteristic G/AXXXG/A motifs spanning across the TM regions (Figure 2A). Previous reports highlight that the interactions among TM domain-containing proteins are mediated by intramolecular and intermolecular hydrogen bonds formed between conserved G/AXXXG/A motifs (Kleiger *et al.*, 2002; Melnyk *et al.*, 2004; Demishtein-Zohary *et al.*, 2015; Demishtein-Zohary *et al.*, 2017; Matta *et al.*, 2017). To understand the role of Mgr2 in regulating the TIM23 complex activity, we performed site-directed mutagenesis to replace amino acids from glycine/alanine to leucine in conserved G/AXXXG/A motifs from TM regions of Mgr2 (Figure 2, A and B). The growth phenotype of the *mgr2* mutants assessed by spotting 10-fold serially diluted wild-type or mutant cells on indicated nonfermentable media (Gebert *et al.*, 2012). Interestingly, three mutants from tandem GXXXG motifs of the Mgr2 TM1 region, namely, $mgr2_{G26L}$, $mgr2_{G30L,}$ and $mgr2_{G34L}$, exhibited severe growth defect at 37°C in both glycerol and lactate media (Figure 2C). However, two mutants from the TM1 region, namely, $mgr2_{G22L}$ and $mgr2_{G39L}$, did not exhibit a temperature-sensitive phenotype (Supplemental Figure S3A). Additionally, the single mutants generated from the TM2 region did not show any growth sensitivity at all the temperatures tested (Figure 2C). Therefore, to ascertain the role of the Mgr2 TM2 region, we generated a combination of double mutants by amino acid substitutions in the GXXXA/GXXXG motifs of the TM2 region. Intriguingly, three mutants, namely, $mgr2_{G57L/A61L}$, $mgr2_{A61L/G65L}$, and $mgr2_{G57L/G68L}$, exhibited growth sensitivity at 37°C in lactate media. At the same time, these mutants did not show any sensitivity in glycerol media, thus indicating that the TM2 region might have a less prominent role compared with the TM1 region in facilitating Mgr2 functions (Figure 2C). Together, these results highlight the conserved functions of TM regions of Mgr2 for cellular viability.

TM1 region is essential for Mgr2 stability

To determine the importance of Mgr2 TM regions in the stability of protein, we analyzed the steady-state levels in all the *mgr2* Ts mutants. Surprisingly, as compared with wild type, Mgr2 TM1 mutants expressed at very low levels and remained undetected by the western analysis (Figure 3A). On the contrary, Mgr2 TM2 mutants showed equivalent levels of expression with that of wild type (Figure 3B). However, the levels of other components of the TIM23 complex remained unaltered in all mutants (Figure 3, A and B). To eliminate the possibility of growth defect due to reduced steady-state levels, we overexpressed Mgr2 TM1 mutants under the control of the centromeric plasmid with a *GPD* promoter. Even after the restoration of protein levels to wild type, all mutants from the TM1 region displayed severe growth defects, thus indicating that the observed growth sensitivity is a consequence of intrinsic functional defects of the mutant proteins (Figure 3, C and D). To gain insights, the half-life of Mgr2 mutant proteins was measured after inhibiting the protein translation by cycloheximide. Surprisingly, all the TM1 mutants displayed accelerated decay in Mgr2 protein levels as a function of time compared with wild type (Figure 3E). In contrast, TM2 mutants exhibited comparable Mgr2 levels to that of wild type at all the time intervals analyzed (Figure 3E). ROMO1, the human orthologue of Mgr2, is a highly unstable protein with a tendency to degrade within 1 h and thus possesses a rapid protein turnover rate (Richter *et al.*, 2019). In agreement, our results indicate that the tandem GXXXG motifs of TM1 region are critical for maintaining the stability of the Mgr2 and mutations in these motifs result in reduced half-life, thus further emphasizing the rapid protein turnover rate associated with the protein.

TM1 region of Mgr2 is critical for association with the TIM23 complex

To determine the Mgr2 TM1 region's role in the assembly of the TIM23 complex, we performed Co-IP in $mgr2_{G26L}$ mutant (TM1 region) using $Tim23_{HA}$ and analyzed the recruitment of different subunits to the core channel by immunodecoration. Surprisingly, copurification of Mgr2 with Tim23 significantly abolished in TM1 mutant (Figure 4A). This further impaired the association of Tim21 since Mgr2 is known to recruit Tim21 to the channel (Figure 4A). Additionally, a significant reduction in copurification of respiratory complex components CytC1 and CoxIV (complex III and IV, respectively) with the TIM23 complex is observed, suggesting a defective bridging between the TIM23 complex and respiratory pathways (Figure 4A). In contrast, the copurification of Tim17, Tim50, Tim44, Pam18, and Pam16 with Tim23 remained unaffected (Figure 4A). Moreover, as negative controls, Co-IP with $Tim23_{HA}$ did not purify Tom70 and Tim9 (which belong to TOM complex and TIM22 complex, respectively), thus confirming the specificity of defects associated with *mgr2* TM1 mutant (Figure 4A).

Besides, we performed Co-IP with $Tim21_{HA}$ to establish a direct role of the Mgr2 TM1 region in bridging the Tim21 and respiratory complexes. Surprisingly, a 50% reduction in the Mgr2 association with Tim21 is observed in TM1 mutant as compared with wild type. At the same time, Tim21 exhibited defective association with core components Tim23, Tim17, and Tim50 (Figure 4B). However, the copurification of CoxIV and CytC1 with Tim21 was found comparable

FIGURE 1: Analysis of Mgr2 interaction with Tim23. (A) The specificity of purified $Tim23_{HIS,}$ GST, and GST-Mgr2 proteins confirmed by immunoblotting using indicated antibodies. (B) In vitro GST–pull-down assay. Immobilized GST-Mgr2 (5 μM) incubated with an increasing concentration of full-length $Tim23_{HIS}$. The bound proteins were subjected to immunoblotting. GST alone was used as a negative control ($n = 3$ per group); 25% of the total sample served as a loading control (input: 25% $Tim23_{HIS}$). (C, D) Triton X–100-lysed mitochondrial extracts were incubated with 5 μM GST or GST-Mgr2 protein for 2 h followed by pull down using anti-GST or anti-HA ($Tim21_{HA}$) antibodies. Immunoblotting was performed using indicated specific antibodies. Input, 10% of the total sample ($n = 3$ per group). (E) Mitochondria solubilized in 1% digitonin buffer subjected to Co-IP using Tim23 antibody–cross-linked beads, followed by immunoblot analysis. Input, 10% of the total sample ($n = 3$ per group). (F) In vitro GST–pull-down assay. Immobilized Mgr2-GST (5 μM) was incubated with an increasing concentration of wild-type $Tim23_{HIS}$ or $Tim23_{HIS}$-G149E. The bound proteins were subjected to immunoblotting ($n = 3$ per group). GST alone served as a negative control. Input: 25% of $Tim23_{HIS}$.

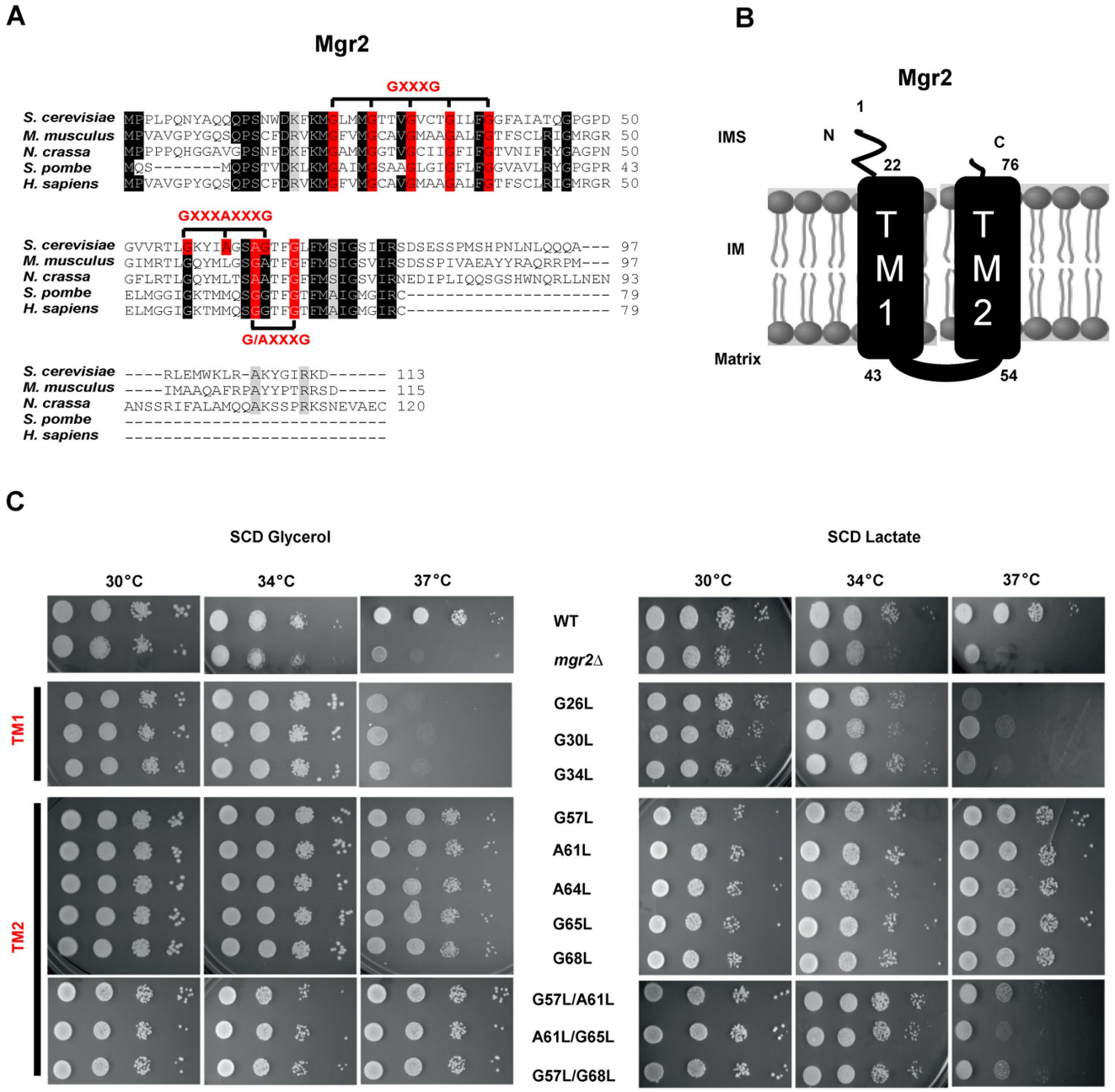

FIGURE 2: Isolation of Ts mutants from Mgr2 TM regions. (A) Sequence alignment of Mgr2 protein across species. Orthologous Mgr2 sequences from different species, including *Saccharomyces cerevisiae*, *Mus musculus*, *Neurospora crassa*, *Schizosaccharomyces pombe*, and *Homo sapiens* were aligned using ClustalW online tool. The sequence corresponding to the G/AXXXG/A motifs are highlighted in red. (B) Modular representation of Mgr2 protein indicating the position of TM regions. (C) Growth phenotype analysis. Wild-type and *mgr2* mutant yeast strains were grown until mid-log phase. The harvested yeast cells were subjected to 10-fold serial dilution followed by spotting on indicated media. Images were captured at identical exposures after 72 h. SCD, synthetic complete defined.

to wild type, indicating that the Tim21 association with respiratory complexes was unaltered (Figure 4B). Moreover, in agreement with the earlier reports, Co-IP with $Tim21_{HA}$ did not purify any subunits of $TIM23^{MOTOR}$ complex, including Tim44, Pam18, and Pam16 (Figure 4B) (Gebert *et al.*, 2012). As negative controls, Tom70 and Tim9 did not copurify with $Tim21_{HA}$ (Figure 4B). In summary, we conclude that the TM1 region of Mgr2 is required for association with Tim23 and Tim21. Further, tandem GXXXG motifs of the Mgr2 TM1 region may act as a stable anchor between Tim23 and Mgr2 through helix–helix packing.

TM2 region of Mgr2 aids in bridging respiratory complexes to the TIM23 complex

To address the importance of the Mgr2 TM2 region, we performed Co-IP with $Tim23_{HA}$ in $mgr2_{G57L/A61L}$ mutant (TM2 region). Strikingly, Mgr2 was efficiently purified with Tim23 similar to wild type (Figure 4C). This indicates that the mutation in the TM2 region does not affect the coupling of Mgr2 to the TIM23 complex. Further, the Mgr2 TM2 mutant displayed significant impairment in the association of Tim21 and defective bridging of CoxIV and CytC1 to the TIM23 complex, indicating that the TM2 region of Mgr2 plays a

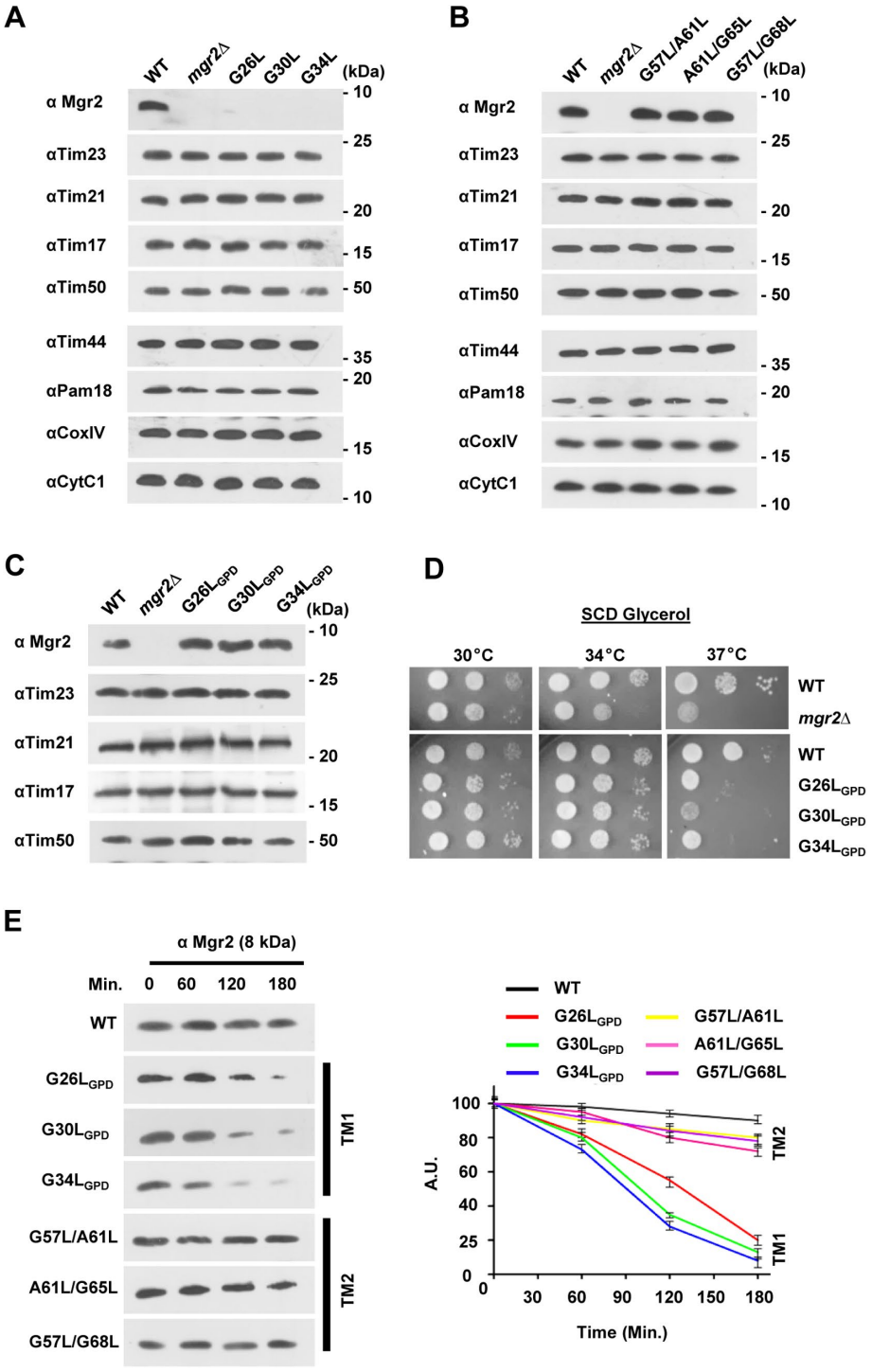

FIGURE 3: Mutation in the TM1 region affects Mgr2 protein stability. (A, B) Steady-state protein levels of the wild-type and *mgr2* mutants (from TM1 and TM2) were analyzed. Samples were divided into two identical sets, separated on Tricine–SDS–PAGE followed by immunoblotting using specific antibodies for different subunits of the TIM23 complex, and respiratory complexes III, IV. (C) Steady-state protein levels of the wild type and *mgr2* mutants (from TM1 region) after overexpression analyzed as described above. (D) The growth phenotype of *mgr2* TM1 mutants overexpressing Mgr2 under the control of the plasmid with centromeric *GPD* promoter analyzed by serial dilution assay as described in Figure 2C. (E) Analysis of protein half-life. The wild-type and mutant yeast cells were grown up to mid-log phase followed by treatment with cycloheximide (50 μg/ml) to inhibit the protein translation. The cells were harvested at different time intervals and subjected to immunoblot analysis. Signals were quantified and represented in a graph (AU, arbitrary units), $n = 3$ per group; ± SE error bars.

distinct role in recruiting Tim21 to the TIM23 complex (Figure 4C). However, the association of Tim23 with core subunits Tim17, Tim50, and import motor components Tim44, Pam18, and Pam16 remained unaltered in TM2 mutant (Figure 4C). At the same time, the specificity of Co-IP was confirmed by immunodecoration against Tom70 and Tim9 (Figure 4C). To further validate the above findings, we analyzed the copurification of translocase components with Tim21$_{HA}$. In agreement with the above findings, the association of Mgr2 with Tim21 was significantly impaired, which consecutively leads to the defective bridging of respiratory complexes with the TIM23 complex (Figure 4D). However, the respiratory complex components CoxIV and CytC1 were purified to a similar extent with Tim21 in wild type and TM2 mutant (Figure 4D). As expected, Co-IP with Tim21$_{HA}$ failed to purify Tim44, Pam18, Pam16, Tom70, and Tim9 (Figure 4D). In summary, the TM2 region of Mgr2 is required for Tim21 binding and thus assists in the assembly of the TIM23^{SORT} complex and the efficient tethering of respiratory complexes, thereby rendering protein import through the TIM23 complex less vulnerable for subtle changes in the inner membrane potential.

Mutation in TM regions of Mgr2 impairs lateral sorting of preproteins

Mgr2 acts as a quality control check for proper biogenesis of membrane proteins by delaying their lateral release into the inner membrane (Ieva *et al.*, 2014). Therefore, to elucidate the role of Mgr2 TM regions in lateral sorting, we performed in vitro import analysis. For the import, we utilized the purified precursor protein Cyb2(167)-dihydrofolate reductase (DHFR), which comprises the mouse DHFR fused to the N-terminal 167 amino acids of cytochrome b2 with an inner membrane-sorting signal and thus localizes to the inner membrane (Geissler *et al.*, 2000; Pareek *et al.*, 2013). Mitochondria isolated from *mgr2* mutants incubated with saturating amounts of Cyb2(167)-DHFR and the import kinetics were monitored by immunoblotting using specific antibodies against DHFR. Strikingly, *mgr2* mutants from both TM regions showed a severe defect in the lateral sorting of preprotein into the inner membrane compared with wild type (Figure 5, A–D). Mgr2 selectively controls the lateral release of the preproteins from the TIM23 complex into the inner membrane by binding to the sorting signal of transiting preprotein, and defective binding leads to the missorting of preprotein into the matrix. However, import into the

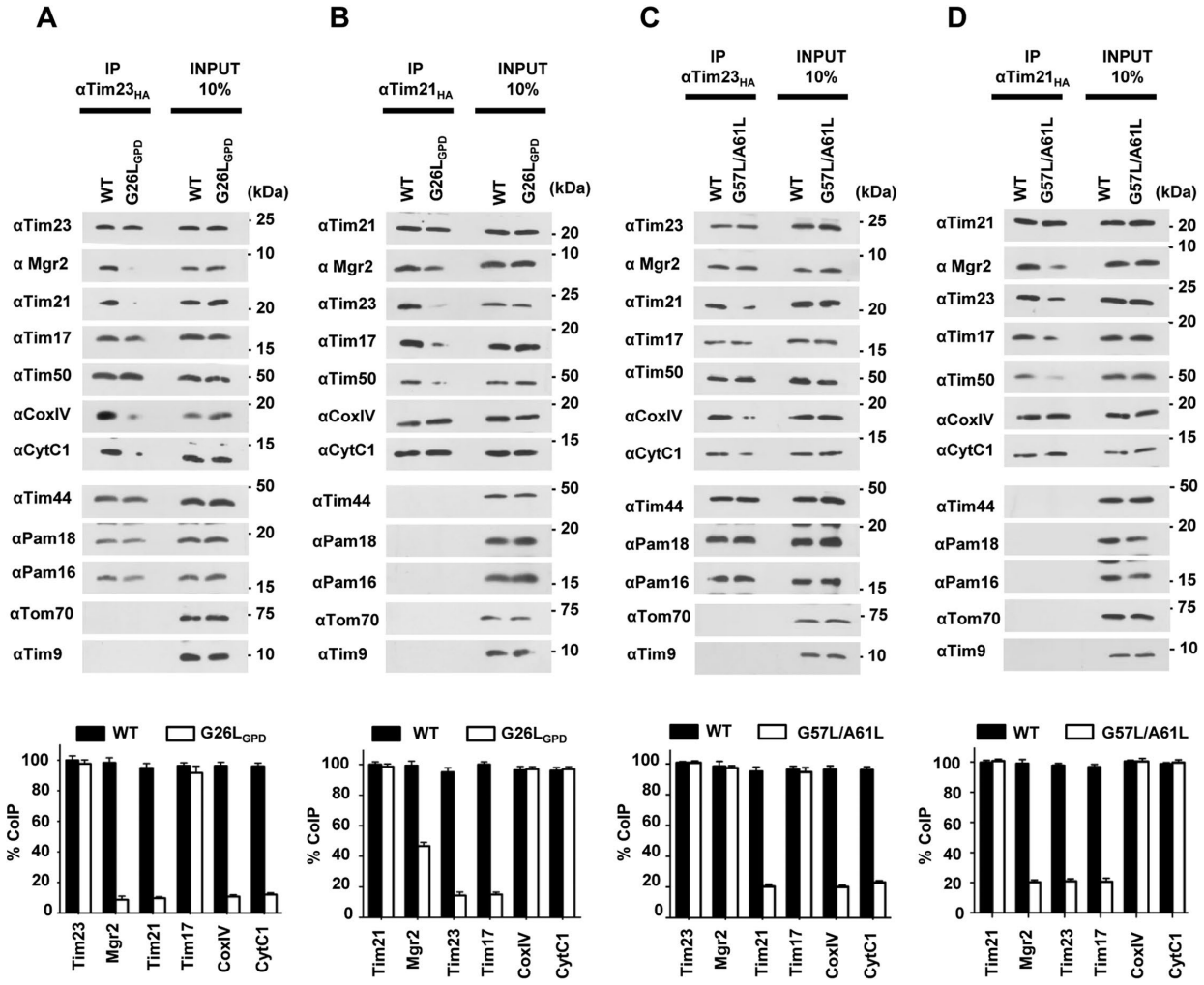

FIGURE 4: Both TM regions of Mgr2 are critical for the assembly of TIM23^{SORT} complex. (A–D) Analysis of TIM23 complex assembly. Mitochondria from the wild-type and *mgr2* TM mutants were lysed with 1% digitonin buffer and subjected to Co-IP using anti-HA antibodies. Samples were divided into two identical sets, separated on Tricine–SDS–gels, followed by immunodecoration with specific antibodies to detect different components of TIM23 complex and respiratory complexes; 10% of the total sample served as a loading control (input). Tom70 and Tim9 were used as negative controls. Signals for immunoprecipitated proteins (Tim23, Mgr2, Tim21, Tim17, CoxIV, and CytC1) were quantified by ImageJ software. ($n = 3$ per group; ± SE error bars).

matrix remains active despite the absence of Mgr2 (Ieva *et al.*, 2014). Similarly, a mutation in either of the TM regions of Mgr2 might have affected its ability to recognize and bind with the sorting signal of inner membrane-sorted preprotein in the TIM23 complex leading to impaired lateral sorting (Figure 5, A–D). At the same time, the deletion of Tim21 was shown to have no defect in the lateral sorting of preproteins (Chacinska *et al.*, 2005). We speculate that the impairment in the lateral sorting observed in *mgr2* TM2 mutant, which is defective solely in Tim21 recruitment, could be attributable to structural rearrangements in the TIM23-channel due to the presence of Mgr2 mutant. Additionally, to examine the role of Mgr2 TM regions in preprotein import into the matrix, we measured the import kinetics using Cyb2(167)Δ19-DHFR (localizes to the matrix) in *mgr2* mutants. Interestingly, preprotein import into the matrix compartment in *mgr2* TM mutants was not significantly impaired compared with wild type (Supplemental Figure S3, B–E), indicating that association of MOTOR components with the TIM23 complex is sufficient to promote preprotein import into the matrix compartment in mgr2 mutants as compared with the complete loss of Mgr2, which was shown to affect matrix import (Gebert *et al.*, 2012). Nevertheless, together, these results indicate that defective association of Mgr2 with Tim23 or the presence of mutant Mgr2 at the TIM23 channel impairs lateral sorting of preproteins into the inner membrane of mitochondria.

Loss of *mgr2* causes aberrations in Mgm1 import leading to fragmentation of the mitochondrial network (Ieva *et al.*, 2014). Similarly, in humans, ROMO1 knockdown results in mitochondrial fragmentation due to defective processing of OPA1 (Mgm1 orthologue) (Norton *et al.*, 2014; Swarnabala *et al.*, 2014; Richter *et al.*, 2019). Since Ts mutants of *mgr2* exhibit impairment in the preprotein import into the inner membrane, we checked the mitochondrial morphology by fluorescence imaging using MTS-mCherry labeling. Interestingly, both mutants showed mitochondrial fragmentation similar to *mgr2*Δ cells as compared with reticular mitochondrial network structures observed for the wild type (Figure 5E). In summary, these results indicate that the TM regions of Mgr2 play a critical role in the proper biogenesis of the inner membrane proteins, which includes several fusion–fission-associated proteins and thus regulate the structural dynamics of mitochondria.

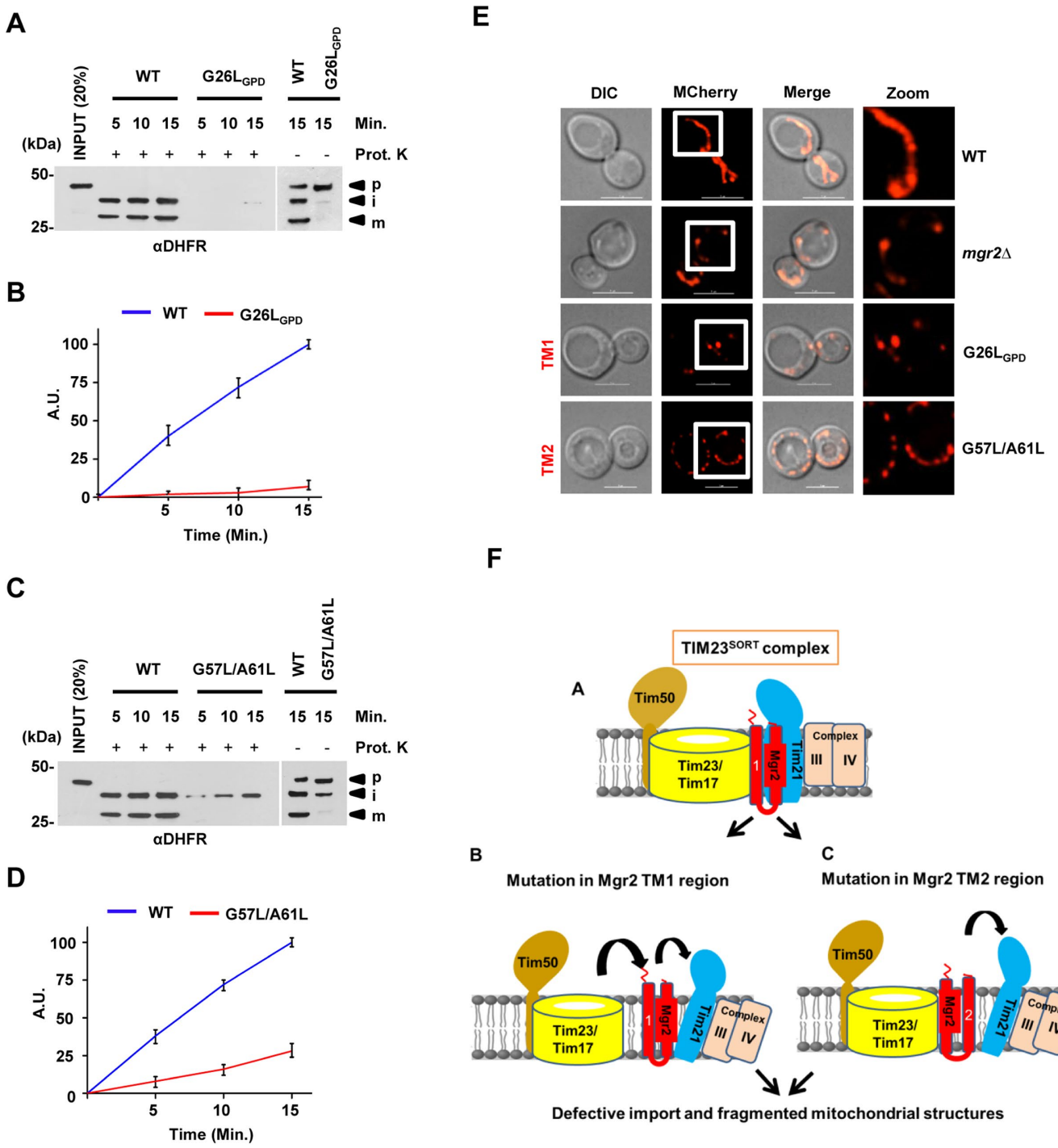

FIGURE 5: Mgr2 TM regions regulate inner membrane sorting and mitochondrial structures. (A–D) In vitro import kinetic analysis. Purified cytb2 (1–167)-DHFR imported into mitochondria were isolated from yeast cells grown at 37°C, followed by PK treatment where indicated. The samples were subsequently analyzed by immunoblotting using an anti-DHFR antibody; p, precursor; i, intermediate; m, mature. The signals were quantified using ImageJ software and represented in the graph after normalizing precursor imported in the wild type at 15 min as 100% import ($n = 3$ per group; ± SE error bars). (E) Analysis of mitochondrial morphology. Wild-type and *mgr2* mutant strains were transformed with MTS-mCherry construct and grown to mid-log phase at 30°C. The samples collected after inducing Ts phenotype and images captured using a Delta Vision Elite fluorescence microscope. Scale bars, 5 μm ($n = 20$ cells per yeast strain). (F) A schematic representation highlighting the role of Mgr2 TM regions. (A) Mgr2 directly associates with channel-forming protein Tim2 and thereby aids in the assembly of the TIM23^{SORT} complex. (B) TM1 region of Mgr2 is critically required for its recruitment to the TIM23 complex. Additionally, the TM1 region also mediates interaction with Tim21. (C) TM2 region of Mgr2 plays a specific role in coupling respiratory complexes to the TIM23 complex via Tim21.

Conclusions

Our current study highlights the role of Mgr2 TM regions in mediating association with Tim23 and provides supporting evidence for the previously proposed models of Mgr2 acting at proximity to the import channel to regulate quality control of preproteins (Figure 5F). Intriguingly, a mutation in either TM region of Mgr2 resulted in defective import into the inner mitochondrial membrane. Moreover, our microscopic analysis revealed that mutation in Mgr2 TM regions leads to altered mitochondrial morphology with significant accumulation of fragmented, mitochondrial structures. Previously, the human orthologue ROMO1 was found differentially regulated in multiple tumor types. Besides, functional defects in ROMO1 are also associated with bone marrow failure, diabetes, and stroke, thereby highlighting the significance of ROMO1 in the regulation of mitochondrial function and health (Chung *et al.*, 2006, 2008, 2012; Shin *et al.*, 2013; Kim *et al.*, 2014, 2017). Therefore, the current discovery is an important contribution in bridging a key lacuna in the field in terms of understanding how Mgr2 regulates the mitochondrial biogenesis and overall cellular physiology, thus serving as a basic platform to further investigate the pathophysiology associated with ROMO1 in humans.

MATERIALS AND METHODS

Yeast strains and plasmid constructions

All the yeast strains used in this study are listed in Supplemental Table S1. Briefly, the haploid mgr2Δ strain is generated by disrupting the *MGR2* gene under W303 yeast background using homologous recombination with hphNT1 cassette, consisting of short flanking regions homologous to *MGR2* loci. For mutagenic analysis, the *MGR2* gene from positions −500 to +500 was PCR amplified using genomic DNA as a templet and cloned into a pRS314 vector. This plasmid was used as a template for further genetic manipulations. The required point mutants of mgr2 were generated by performing site-directed mutagenesis with high-fidelity Pfu-Turbo polymerase (Stratagene) using appropriate primers. The mutant mgr2 plasmids were transformed into mgr2Δ strain and the growth phenotype was monitored by spotting them on auxotrophic synthetic-defined medium lacking the respective selection marker and incubation at different temperatures. All tim23 strains used in this study were previously generated (Pareek *et al.*, 2013).

Mitochondrial isolation

Isolation of mitochondria was performed similarly to previously published protocols (Meisinger *et al.*, 2006; Pareek *et al.*, 2013; Schendzielorz *et al.*, 2018). Wild-type and mutant yeast cells were grown in YPG medium at 30°C (if not indicated otherwise) until optical density reached 2. The cells were harvested and treated with 10 mM DTT in buffer containing 100 mM Tris-H_2SO_4 (pH 9.4) for 30 min at 30°C. After washing twice, the cells were incubated in zymolyase buffer (20 mM KPO_4, pH 7.4, 1.2 M sorbitol, and 0.57 mg/l zymolyase) for 1 h at 30°C for cell wall lysis. The resulting spheroplasts were homogenized in ice-cold homogenization buffer (600 mM sorbitol, 10 mM Tris-HCl, pH 7.4, 1 g/l BSA, 1 mM phenylmethylsulfonyl fluoride [PMSF], and 1 mM EDTA) followed by a combination of differential centrifugation steps to obtain the pure mitochondrial fraction. Isolated mitochondria were resuspended in SEM buffer (10 mM MOPS-KOH, pH 7.2, 250 mM sucrose, 1 mM EDTA), frozen in liquid nitrogen, and stored at −80°C.

Co-IP

The mitochondria from wild-type and mutant mgr2 strains expressing HA-tagged Tim23 or Tim21 were isolated from cells grown at 37°C. The Co-IP was performed by lysing mitochondria in the buffer (50 mM Tris-HCl, pH 7.4, 10% glycerol, 80 mM KCl, 5 mM EDTA, and 1 mM PMSF) containing 1% digitonin for 45 min at 4°C. The lysates were subjected to centrifugation and the resulting supernatant was incubated with anti-HA-bound protein G-Sepharose beads for 1 h at 4°C. Subsequently, the beads were washed with the same lysis buffer, and the samples were separated on Tricine–SDS–PAGE followed by immunoblotting using specific antibodies. In the case of tim23 mutants, Co-IP was performed using affinity-purified Tim23 antibodies coupled to protein A-sepharose beads by dimethyl pimelimidate cross-linker.

Import kinetics analysis

Purified precursor proteins Cyb2(1–167)-DHFR and Cyb2(1–167)Δ19-DHFR were used to perform in vitro import kinetics as reported previously (Geissler *et al.*, 2000; Pareek *et al.*, 2013; Matta *et al.*, 2017). Isolated mitochondria were incubated with precursor proteins in import buffer (250 mM sucrose, 10 mM MOPS/KOH pH 7.2, 80 mM KCl, 2 mM KH_2PO_4, 5 mM dithiothreitol,5 mM $MgCl_2$, 3% fatty acid-free BSA, 2 mM ATP, and 2 mM NADH) at 25°C for 5, 10, or 15 min. The import reaction was stopped by dissipating mitochondrial membrane potential using 1 μM valinomycin (Sigma). Samples were treated with 0.1 mg/ml proteinase K (PK) to remove nonimported precursor proteins for 20 min on ice, followed by 1 mM PMSF (US Biological) treatment to inactivate PK. Resulting samples were washed twice with SEM buffer (250 mM sucrose, 20 mM MOPS, pH 7.2, and 1 mM EDTA) and separated on SDS–PAGE, and immunoblotting was performed to detect the import of preproteins.

Protein expression and purification

GST-tagged Mgr2 purification. The DNA sequence corresponding to mature Mgr2 protein (devoid of C-terminal targeting sequence) was cloned into the pGEX-KG vector and expressed in an *Escherichia coli* (BL21) strain. The cells were allowed to grow at 25°C until the mid-log phase, followed by 8 h induction using 1 mM IPTG (isopropyl 1-thio-β-D-galactopyranoside). The cells were harvested and the lysate was prepared by treating with 0.2 mg/ml lysozyme at 4°C for 1 h in buffer A (50 mM Tris-Cl, pH 7.5, 100 mM NaCl, 1 mM dithiothreitol, 0.5 mM EDTA, 1 mM PMSF, and 10% glycerol). The lysate was further incubated with 0.2% deoxycholate, followed by DNase I (10 μg/ml) treatment for 15 min at 4°C. Subsequently, the supernatant was collected by centrifugation at 22,000 × *g* for 45 min at 4°C, followed by incubation with pre-equilibrated GST-sepharose beads for 2 h at 4°C. Beads were washed with buffer B (Buffer A + 0.2% Triton X-100) multiple times to eliminate any residual contamination. Finally, the protein-bound beads were resuspended in buffer containing 50 mM Tris-Cl, pH 7.5, and 100 mM NaCl and stored at 4°C.

Purification of Tim23 protein. Purification of Tim23 was performed according to a previously published method (Pareek *et al.*, 2013). Briefly, the *TIM23* ORF was PCR amplified and cloned into a pRSF-Duet-1 expression vector. This construct was transformed into *E. coli* (RIL) cells and grown until the mid-log phase at 37°C; 1 mM IPTG was added to the culture for protein induction and incubated for 5 h at 37°C. Harvested cells were lysed in lysis buffer (20 mM Na-phosphate, pH 7.5, 20 mM Imidazole, 100 mM NaCl, 10% glycerol, and 1 mM PMSF); 0.2 mg/ml lysozyme were added and incubated at 4°C for 45 min with constant mixing. The lysates were subjected to gentle treatment with 0.2% deoxycholate, followed by DNase I (10 μg/ml) for 15 min at 4°C. Pellet and supernatant fractions were separated by centrifugation at 22,000 × *g*. Tim23 protein was recovered

from the reconstitution of inclusion bodies before being subjected to purification using Ni-NTA chromatography.

GST pull-down analysis

In vitro pull-down assay. Mgr2-GST protein was immobilized on beads equilibrated with buffer A (50 mM Tris-Cl, pH 7.5, 100 mM NaCl, 0.1% Triton X-100, 10% glycerol) followed by blocking the beads with 0.2% BSA for 30 min. Excess BSA was removed by washing the beads with buffer A (three times). Subsequently, beads were resuspended in buffer A and incubated with an increasing concentration of Tim23 protein for 2 h at 4°C. Finally, the beads were washed with buffer A three times to eliminate nonspecific binding. The samples were prepared and resolved on SDS–PAGE, followed by immunoblotting using specific antibodies.

In vivo pull-down assay. Isolated mitochondria were solubilized in buffer B (50 mM Tris-Cl, pH 7.5, 150 mM NaCl, 5 mM EDTA, 2 mM PMSF, 0.1% Triton X-100, 10% glycerol) and the lysates were subjected to centrifugation at 22,000 × *g* at 4°C for 15 min. The supernatant lysates were incubated with GST- Mgr2 protein for 2 h followed by pull down using anti-GST or anti-HA ($Tim21_{HA}$) antibodies. After washing the protein-bound beads with buffer B (three times), samples were eluted and separated on Tricine–SDS–PAGE followed by immunoblotting using specific antibodies.

Analysis of mitochondrial morphology

Visualization of mitochondrial morphology was performed as per previously published protocols (Matta *et al.*, 2017). Briefly, wild-type and mutant yeast cells were transformed with a pRS415 vector containing the presequence of subunit 9 followed by an mCherry fluorescent protein, which allows it to translocate and decorate the mitochondria. The cells were harvested after growing until the mid-log phase and washed with 1× phosphate-buffered saline. Subsequently, cells were mounted on agarose pads with Antifade (Invitrogen), and a Delta Vision Elite fluorescence microscope (GE Healthcare) with a 100× objective lens was used to acquire images. Images were deconvolved and analyzed using SoftWoRx 6.1.3. Software.

Statistical analyses

Error bars represent standard errors (± SE) derived from three independent experiments. Significance was tested by one-way analysis of variance and Dunnett's multiple-comparison posttest; $p < 0.05$ was considered significant. The intensity of individual bands was quantified by densitometry using ImageJ software.

Miscellaneous

Tricine polyacrylamide gels were prepared as reported earlier for the resolution of proteins below 15 kDa (Schagger, 2006; Richter *et al.*, 2019). The antisera used for yeast-specific Mgr2 was a kind gift from Nikolaus Pfanner (Universität Freiburg, Germany) (Ieva *et al.*, 2014). The antisera used for immunodecoration against yeast-specific proteins such as Tim23, Tim17, Tim50, Tim44, Tim9, GST, Pam18, and Pam16 was raised in rabbits, as reported earlier (Pareek *et al.*, 2013; Matta *et al.*, 2017). Chemicals used in the study were obtained from Sigma-Aldrich if not specified. All immunoblot analyses were performed using an enhanced chemiluminescence system (PerkinElmer) according to the manufacturer's instructions.

ACKNOWLEDGMENTS

We are grateful to Nikolaus Pfanner and Martin van der Laan, Universität Freiburg, Germany, for providing anti-Mgr2 antibody. We thank Elizabeth A Craig, University of Wisconsin—Madison for providing the anti-Tim44 antibody. This work was supported by the Swarnajayanthi Fellowship (DST/SJF/LS-01/2011–2012), Department of Biotechnology (DBT-IISC Partnership Program Phase-II [No. BT/PR27952/IN/22/212/2018] and DST-FIST Programme-Phase III [No. SR/FST/LSII-045/2016(G)] to P.D.S. S.K.M. acknowledges a research fellowship from the University Grants Commission. A.K. acknowledges a research fellowship from the Council of Scientific and Industrial Research.

REFERENCES

Albrecht R, Rehling P, Chacinska A, Brix J, Cadamuro SA, Volkmer R, Guiard B, Pfanner N, Zeth K (2006). The Tim21 binding domain connects the preprotein translocases of both mitochondrial membranes. EMBO Rep 7, 1233–1238.

Alder NN, Jensen RE, Johnson AE (2008). Fluorescence mapping of mitochondrial TIM23 complex reveals a water-facing, substrate-interacting helix surface. Cell 134, 439–450.

Araiso Y, Tsutsumi A, Qiu J, Imai K, Shiota T, Song J, Lindau C, Wenz LS, Sakaue H, Yunoki K, *et al.* (2019). Structure of the mitochondrial import gate reveals distinct preprotein paths. Nature 575, 395–401.

Bajaj R, Jaremko L, Jaremko M, Becker S, Zweckstetter M (2014). Molecular basis of the dynamic structure of the TIM23 complex in the mitochondrial intermembrane space. Structure 22, 1501–1511.

Baker MJ, Frazier AE, Gulbis JM, Ryan MT (2007). Mitochondrial protein-import machinery: correlating structure with function. Trends Cell Biol 17, 456–464.

Banerjee R, Gladkova C, Mapa K, Witte G, Mokranjac D (2015). Protein translocation channel of mitochondrial inner membrane and matrix-exposed import motor communicate via two-domain coupling protein. Elife 4, e11897.

Bauer MF, Sirrenberg C, Neupert W, Brunner M (1996). Role of Tim23 as voltage sensor and presequence receptor in protein import into mitochondria. Cell 87, 33–41.

Berthold J, Bauer MF, Schneider HC, Klaus C, Dietmeier K, Neupert W, Brunner M (1995). The MIM complex mediates preprotein translocation across the mitochondrial inner membrane and couples it to the mt-Hsp70/ATP driving system. Cell 81, 1085–1093.

Chacinska A, Koehler CM, Milenkovic D, Lithgow T, Pfanner N (2009). Importing mitochondrial proteins: machineries and mechanisms. Cell 138, 628–644.

Chacinska A, Lind M, Frazier AE, Dudek J, Meisinger C, Geissler A, Sickmann A, Meyer HE, Truscott KN, Guiard B, *et al.* (2005). Mitochondrial presequence translocase: switching between TOM tethering and motor recruitment involves Tim21 and Tim17. Cell 120, 817–829.

Chung JS, Park S, Park SH, Park ER, Cha PH, Kim BY, Chung YM, Woo SR, Han CJ, Kim SB, *et al.* (2012). Overexpression of Romo1 promotes production of reactive oxygen species and invasiveness of hepatic tumor cells. Gastroenterology 143, 1084–1094.e1087.

Chung YM, Kim JS, Yoo YD (2006). A novel protein, Romo1, induces ROS production in the mitochondria. Biochem Biophys Res Commun 347, 649–655.

Chung YM, Lee SB, Kim HJ, Park SH, Kim JJ, Chung JS, Yoo YD (2008). Replicative senescence induced by Romo1-derived reactive oxygen species. J Biol Chem 283, 33763–33771.

D'Silva P, Liu Q, Walter W, Craig EA (2004). Regulated interactions of mtHsp70 with Tim44 at the translocon in the mitochondrial inner membrane. Nat Struct Mol Biol 11, 1084–1091.

D'Silva PR, Schilke B, Hayashi M, Craig EA (2008). Interaction of the J-protein heterodimer Pam18/Pam16 of the mitochondrial import motor with the translocon of the inner membrane. Mol Biol Cell 19, 424–432.

D'Silva PD, Schilke B, Walter W, Andrew A, Craig EA (2003). J protein cochaperone of the mitochondrial inner membrane required for protein import into the mitochondrial matrix. Proc Natl Acad Sci USA 100, 13839–13844.

D'Silva PR, Schilke B, Walter W, Craig EA (2005). Role of Pam16's degenerate J domain in protein import across the mitochondrial inner membrane. Proc Natl Acad Sci USA 102, 12419–12424.

Dayan D, Bandel M, Gunsel U, Nussbaum I, Prag G, Mokranjac D, Neupert W, Azem A (2019). A mutagenesis analysis of Tim50, the major receptor of the TIM23 complex, identifies regions that affect its interaction with Tim23. Sci Rep 9, 2012.

de la Cruz L, Bajaj R, Becker S, Zweckstetter M (2010). The intermembrane space domain of Tim23 is intrinsically disordered with a distinct binding region for presequences. Protein Sci 19, 2045–2054.
De Los Rios P, Ben-Zvi A, Slutsky O, Azem A, Goloubinoff P (2006). Hsp70 chaperones accelerate protein translocation and the unfolding of stable protein aggregates by entropic pulling. Proc Natl Acad Sci USA 103, 6166–6171.
Dekker PJ, Keil P, Rassow J, Maarse AC, Pfanner N, Meijer M (1993). Identification of MIM23, a putative component of the protein import machinery of the mitochondrial inner membrane. FEBS Lett 330, 66–70.
Demishtein-Zohary K, Gunsel U, Marom M, Banerjee R, Neupert W, Azem A, Mokranjac D (2017). Role of Tim17 in coupling the import motor to the translocation channel of the mitochondrial presequence translocase. Elife 6.
Demishtein-Zohary K, Marom M, Neupert W, Mokranjac D, Azem A (2015). GxxxG motifs hold the TIM23 complex together. FEBS J 282, 2178–2186.
Denkert N, Schendzielorz AB, Barbot M, Versemann L, Richter F, Rehling P, Meinecke M (2017). Cation selectivity of the presequence translocase channel Tim23 is crucial for efficient protein import. Elife 6.
Emtage JL, Jensen RE (1993). MAS6 encodes an essential inner membrane component of the yeast mitochondrial protein import pathway. J Cell Biol 122, 1003–1012.
Frazier AE, Dudek J, Guiard B, Voos W, Li Y, Lind M, Meisinger C, Geissler A, Sickmann A, Meyer HE, *et al.* (2004). Pam16 has an essential role in the mitochondrial protein import motor. Nat Struct Mol Biol 11, 226–233.
Gebert M, Schrempp SG, Mehnert CS, Heisswolf AK, Oeljeklaus S, Ieva R, Bohnert M, von der Malsburg K, Wiese S, Kleinschroth T, *et al.* (2012). Mgr2 promotes coupling of the mitochondrial presequence translocase to partner complexes. J Cell Biol 197, 595–604.
Geissler A, Chacinska A, Truscott KN, Wiedemann N, Brandner K, Sickmann A, Meyer HE, Meisinger C, Pfanner N, Rehling P (2002). The mitochondrial presequence translocase: an essential role of Tim50 in directing preproteins to the import channel. Cell 111, 507–518.
Geissler A, Krimmer T, Bomer U, Guiard B, Rassow J, Pfanner N (2000). Membrane potential-driven protein import into mitochondria. The sorting sequence of cytochrome b(2) modulates the deltapsi-dependence of translocation of the matrix-targeting sequence. Mol Biol Cell 11, 3977–3991.
Geissler A, Rassow J, Pfanner N, Voos W (2001). Mitochondrial import driving forces: enhanced trapping by matrix Hsp70 stimulates translocation and reduces the membrane potential dependence of loosely folded preproteins. Mol Cell Biol 21, 7097–7104.
Ieva R, Schrempp SG, Opalinski L, Wollweber F, Hoss P, Heisswolf AK, Gebert M, Zhang Y, Guiard B, Rospert S, *et al.* (2014). Mgr2 functions as lateral gatekeeper for preprotein sorting in the mitochondrial inner membrane. Mol Cell 56, 641–652.
Kang Y, Fielden LF, Stojanovski D (2018). Mitochondrial protein transport in health and disease. Semin Cell Dev Biol 76, 142–153.
Kim HJ, Jo MJ, Kim BR, Kim JL, Jeong YA, Na YJ, Park SH, Lee SY, Lee DH, Lee HS, *et al.* (2017). Reactive oxygen species modulator-1 (Romo1) predicts unfavorable prognosis in colorectal cancer patients. PLoS One 12, e0176834.
Kim IG, Kim SY, Kim HA, Kim JY, Lee JH, Choi SI, Han JR, Kim KC, Cho EW (2014). Disturbance of DKK1 level is partly involved in survival of lung cancer cells via regulation of ROMO1 and gamma-radiation sensitivity. Biochem Biophys Res Commun 443, 49–55.
Kleiger G, Grothe R, Mallick P, Eisenberg D (2002). GXXXG and AXXXA: common alpha-helical interaction motifs in proteins, particularly in extremophiles. Biochemistry 41, 5990–5997.
Kozany C, Mokranjac D, Sichting M, Neupert W, Hell K (2004). The J domain-related cochaperone Tim16 is a constituent of the mitochondrial TIM23 preprotein translocase. Nat Struct Mol Biol 11, 234–241.
Kubrich M, Keil P, Rassow J, Dekker PJ, Blom J, Meijer M, Pfanner N (1994). The polytopic mitochondrial inner membrane proteins MIM17 and MIM23 operate at the same preprotein import site. FEBS Lett 349, 222–228.
Lee SH, Min JW, Lee JS, Kim CH, Yoo YD, Lee EJ, Min KH, Hur GY, Lee SY, Kim JH, *et al.* (2015). Reactive oxygen species modulator 1 (Romo1) overexpression is an independent predictor of poor survival in NSCLC patients who undergo surgical resection. Lung Cancer 87, 45–52.
Li J, Sha B (2015). The structure of Tim50(164-361) suggests the mechanism by which Tim50 receives mitochondrial presequences. Acta Crystallogr F Struct Biol Commun 71, 1146–1151.
Liu Q, D'Silva P, Walter W, Marszalek J, Craig EA (2003). Regulated cycling of mitochondrial Hsp70 at the protein import channel. Science 300, 139–141.
Maarse AC, Blom J, Keil P, Pfanner N, Meijer M (1994). Identification of the essential yeast protein MIM17, an integral mitochondrial inner membrane protein involved in protein import. FEBS Lett 349, 215–221.
Marom M, Dayan D, Demishtein-Zohary K, Mokranjac D, Neupert W, Azem A (2011). Direct interaction of mitochondrial targeting presequences with purified components of the TIM23 protein complex. J Biol Chem 286, 43809–43815.
Martin J, Mahlke K, Pfanner N (1991). Role of an energized inner membrane in mitochondrial protein import. Delta psi drives the movement of presequences. J Biol Chem 266, 18051–18057.
Martinez-Caballero S, Grigoriev SM, Herrmann JM, Campo ML, Kinnally KW (2007). Tim17p regulates the twin pore structure and voltage gating of the mitochondrial protein import complex TIM23. J Biol Chem 282, 3584–3593.
Matta SK, Pareek G, Bankapalli K, Oblesha A, D'Silva P (2017). Role of Tim17 Transmembrane Regions in Regulating the Architecture of Presequence Translocase and Mitochondrial DNA Stability. Mol Cell Biol 37 27994013, doi:10.1128/MCB.00491-16.
Meier S, Neupert W, Herrmann JM (2005). Conserved N-terminal negative charges in the Tim17 subunit of the TIM23 translocase play a critical role in the import of preproteins into mitochondria. J Biol Chem 280, 7777–7785.
Meisinger C, Pfanner N, Truscott KN (2006). Isolation of yeast mitochondria. Methods Mol Biol 313, 33–39.
Melnyk RA, Kim S, Curran AR, Engelman DM, Bowie JU, Deber CM (2004). The affinity of GXXXG motifs in transmembrane helix-helix interactions is modulated by long-range communication. J Biol Chem 279, 16591–16597.
Mirzalieva O, Jeon S, Damri K, Hartke R, Drwesh L, Demishtein-Zohary K, Azem A, Dunn CD, Peixoto PM (2019). Deletion of Mgr2p Affects the Gating Behavior of the TIM23 Complex. Front Physiol 9, 1960.
Mokranjac D, Paschen SA, Kozany C, Prokisch H, Hoppins SC, Nargang FE, Neupert W, Hell K (2003). Tim50, a novel component of the TIM23 preprotein translocase of mitochondria. EMBO J 22, 816–825.
Mokranjac D, Popov-Celeketic D, Hell K, Neupert W (2005). Role of Tim21 in mitochondrial translocation contact sites. J Biol Chem 280, 23437–23440.
Na AR, Chung YM, Lee SB, Park SH, Lee MS, Yoo YD (2008). A critical role for Romo1-derived ROS in cell proliferation. Biochem Biophys Res Commun 369, 672–678.
Neupert W, Herrmann JM (2007). Translocation of proteins into mitochondria. Annu Rev Biochem 76, 723–749.
Norton M, Ng AC, Baird S, Dumoulin A, Shutt T, Mah N, Andrade-Navarro MA, McBride HM, Screaton RA (2014). ROMO1 is an essential redox-dependent regulator of mitochondrial dynamics. Sci Signal 7, ra10.
Pareek G, Krishnamoorthy V, D'Silva P (2013). Molecular insights revealing interaction of Tim23 and channel subunits of presequence translocase. Mol Cell Biol 33, 4641–4659.
Pfanner N, Warscheid B, Wiedemann N (2019). Mitochondrial proteins: from biogenesis to functional networks. Nat Rev Mol Cell Biol 20, 267–284.
Ramesh A, Peleh V, Martinez-Caballero S, Wollweber F, Sommer F, van der Laan M, Schroda M, Alexander RT, Campo ML, Herrmann JM (2016). A disulfide bond in the TIM23 complex is crucial for voltage gating and mitochondrial protein import. J Cell Biol 214, 417–431.
Richter F, Dennerlein S, Nikolov M, Jans DC, Naumenko N, Aich A, MacVicar T, Linden A, Jakobs S, Urlaub H, *et al.* (2019). ROMO1 is a constituent of the human presequence translocase required for YME1L protease import. J Cell Biol 218, 598–614.
Ryan KR, Menold MM, Garrett S, Jensen RE (1994). SMS1, a high-copy suppressor of the yeast mas6 mutant, encodes an essential inner membrane protein required for mitochondrial protein import. Mol Biol Cell 5, 529–538.
Schagger H (2006). Tricine-SDS-PAGE. Nat Protoc 1, 16–22.
Schendzielorz AB, Bragoszewski P, Naumenko N, Gomkale R, Schulz C, Guiard B, Chacinska A, Rehling P (2018). Motor recruitment to the TIM23 channel's lateral gate restricts polypeptide release into the inner membrane. Nat Commun 9, 4028.
Schendzielorz AB, Schulz C, Lytovchenko O, Clancy A, Guiard B, Ieva R, van der Laan M, Rehling P (2017). Two distinct membrane potential-dependent steps drive mitochondrial matrix protein translocation. J Cell Biol 216, 83–92.
Schiller D (2009). Pam17 and Tim44 act sequentially in protein import into the mitochondrial matrix. Int J Biochem Cell Biol 41, 2343–2349.
Schmidt O, Pfanner N, Meisinger C (2010). Mitochondrial protein import: from proteomics to functional mechanisms. Nat Rev Mol Cell Biol 11, 655–667.

Schulz C, Schendzielorz A, Rehling P (2015). Unlocking the presequence import pathway. Trends Cell Biol 25, 265–275.
Shin JA, Chung JS, Cho SH, Kim HJ, Yoo YD (2013). Romo1 expression contributes to oxidative stress-induced death of lung epithelial cells. Biochem Biophys Res Commun 439, 315–320.
Swarnabala S, Gattu M, Perry B, Cho Y, Lockey RF, Kolliputi N (2014). ROMO1 links oxidative stress to mitochondrial integrity. J Cell Commun Signal 9, 73–75.
Tamura Y, Harada Y, Shiota T, Yamano K, Watanabe K, Yokota M, Yamamoto H, Sesaki H, Endo T (2009). Tim23-Tim50 pair coordinates functions of translocators and motor proteins in mitochondrial protein import. J Cell Biol 184, 129–141.
Ting SY, Yan NL, Schilke BA, Craig EA (2017). Dual interaction of scaffold protein Tim44 of mitochondrial import motor with channel-forming translocase subunit Tim23. Elife 6.
Truscott KN, Brandner K, Pfanner N (2003). Mechanisms of protein import into mitochondria. Curr Biol 13, R326–R337.
Truscott KN, Kovermann P, Geissler A, Merlin A, Meijer M, Driessen AJ, Rassow J, Pfanner N, Wagner R (2001). A presequence- and voltage-sensitive channel of the mitochondrial preprotein translocase formed by Tim23. Nat Struct Biol 8, 1074–1082.
van der Laan M, Hutu DP, Rehling P (2010). On the mechanism of preprotein import by the mitochondrial presequence translocase. Biochim Biophys Acta 1803, 732–739.
van der Laan M, Wiedemann N, Mick DU, Guiard B, Rehling P, Pfanner N (2006). A role for Tim21 in membrane-potential-dependent preprotein sorting in mitochondria. Curr Biol 16, 2271–2276.
Wiedemann N, Pfanner N (2017). Mitochondrial machineries for protein import and assembly. Annu Rev Biochem 86, 685–714.
Wiedemann N, van der Laan M, Hutu DP, Rehling P, Pfanner N (2007). Sorting switch of mitochondrial presequence translocase involves coupling of motor module to respiratory chain. J Cell Biol 179, 1115–1122.
Yamamoto H, Esaki M, Kanamori T, Tamura Y, Nishikawa S, Endo T (2002). Tim50 is a subunit of the TIM23 complex that links protein translocation across the outer and inner mitochondrial membranes. Cell 111, 519–528.
Zarsky V, Dolezal P (2016). Evolution of the Tim17 protein family. Biol Direct 11, 54.